Conductance of carbon nanotubes with disorder: A numerical study

M. P. Anantram*
NASA Ames Research Center, Mail Stop T27A-1, Moffett Field, California 94045-1000

T. R. Govindan†
Applied Research Laboratory, P.O. Box 30, State College, Pennsylvania 16804-0030
(Received 9 March 1998; revised manuscript received 15 May 1998)

We study the conductance of carbon nanotube wires in the presence of disorder, in the limit of phase-coherent transport. For this purpose, we have developed a simple numerical procedure to compute transmission through carbon nanotubes and related structures. Two models of disorder are considered, weak uniform disorder and isolated strong scatterers. In the case of weak uniform disorder, our simulations show that the conductance is not significantly affected by disorder when the Fermi energy is close to the band center. Further, the transmission around the band center depends on the diameter of these zero band-gap wires. We also find that the calculated small bias conductance as a function of the Fermi energy exhibits a dip when the Fermi energy is close to the second subband minima. In the presence of strong isolated disorder, our calculations show a transmission gap at the band center, and the corresponding conductance is very small. [S0163-1829(98)05532-5]

I. INTRODUCTION

The experimental and theoretical study of carbon nanotubes (CNT) has recently been active because these low-dimensional materials display interesting properties both from a fundamental physics and applications viewpoint. The mechanical strength of CNT combined with their rich electronic properties have led to a demonstration of their proposed applications as STM tips,[1] field emission sources,[2] and nanoscale devices.[3–5] CNT can presently be cut to lengths varying from tens of a nanometer to a many micrometers, and experiments have shown promise as molecular wires.[3] On the theoretical side, studies of the conductance of CNT with single defects and a junction between tubes have generated interest,[6–8] as has the low-energy excitation spectrum in the presence of electron-electron interaction.[9–13]

A metallic CNT has two propagating subbands at the Fermi energy. This can yield a maximum low bias conductance of $4e^2/h$ $(6.25k\Omega)$. The prospect of realizing conductances close to $4e^2/h$ will significantly depend on (i) the role of disorder and/or defects in reducing the conductance of this low-dimensional material and (ii) the ability to realize near perfect contacts with macroscopic sized voltage pads. Using numerical simulation, we study the effect of two types of disorder. The first type of disorder is a relatively weak uniform disorder that is distributed throughout the sample. This model has been considered previously in different contexts.[14] The second type of disorder is isolated strong scatterers. These scatterers physically correspond to lattice sites onto which an electron cannot hop easily. We find that the two types of disorder affect the conductance in very different manners. We present the results of our conductance calculations in nanotubes of different lengths and diameters. We also make suggestions to observe some of these results experimentally. The second contribution of our paper is a procedure that can be used for the numerical computation of the transport properties of CNT with defects, *T*, *Y*, and other junctions[15–17] and CNT heterostructures. Our procedure includes the effect of semi-infinite leads in an efficient manner. The Green's-function-based transport formulation of Refs. 18–20 is employed and is applicable to devices with arbitrary disordered regions and junctions.

The paper is organized as follows. We discuss the model and the Green's-function method in Sec. II. This is followed by a discussion of the numerical results in Sec. III. We conclude in Sec. IV.

II. MODEL

The electronic properties of CNT have been calculated in the context of various approximations. We use the simplest model, which assumes the nanotube to be an sp^2 bonded network. The corresponding single-particle Hamiltonian is[21–23]

$$H=\sum_i \epsilon_i^0 c_i^\dagger c_i+\sum_{i,j} t_{ij} c_i^\dagger c_j . \tag{2.1}$$

Here, ϵ_i^0 is the on-site potential and t_{ij} is the hopping parameter between lattice sites i and j. $\{c_i^\dagger, c_i\}$ are the creation and annihilation operators at site i. In the absence of defects, the on-site potential ϵ_i^0 is zero and the hopping parameter is -3.1 eV.[22] We calculate the conductance of a structure that consists of two semi-infinite perfect CNT leads separated by a region with defects (Fig. 1). In the presence of defects, both the on-site potential and the hopping parameter change. Here, we only consider the variation in the on-site potential,



FIG. 1. A schematic representation of the structure across which the transmission is calculated. Our calculation accounts for semi-infinite leads connected to the disordered region.

 © 1998 The American Physical Society

$$\epsilon_i^0 \rightarrow \epsilon_i^0 + \delta\epsilon_i . \tag{2.2}$$

In the case of a uniformly distributed weak disorder, $\delta\epsilon_i$ is randomly chosen from the interval $\pm|\epsilon_{\text{random}}|$ at every lattice point. Increasing ϵ_{random} corresponds to increasing the amount of disorder. In the case of substitutional defects, $\delta\epsilon_i$ is set to a large number at some random lattice sites. In a real sample, $\delta\epsilon_i$ would be expected to have a finite spatial extent. In this paper, the finite spatial extent is neglected and the random component is treated as a δ-function potential.

The transmission coefficient between the left and right leads is calculated using the expression[19,20]

$$T(E) = \mathrm{tr}(\Gamma_L G^r \Gamma_R G^a). \tag{2.3}$$

The coupling of the device to the left and right leads, Γ_L and Γ_R, is given by

$$\Gamma_k(E) = 2\pi V_k^\dagger \mathrm{Im}[g_k^r(E)] V_k, \tag{2.4}$$

where $k \in L,R$. $g_k^r(E)$ is the Green's-function matrix of the kth semi-infinite lead, G^r and G^a are the retarded and advanced Green's-function matrices of the device (including the coupling to the semi-infinite leads), and V_k is the matrix that couples the kth lead to the device (disordered) region. The trace is over the device nodes. To obtain the Green's functions, we solve the following equation:

$$(EI - H - \Sigma_L^r - \Sigma_R^r) G^r = I, \tag{2.5}$$

where $\Sigma_k^r = V_k^\dagger g_k^r (k \in L,R) V_k$ represents the self-energy due to the semi-infinite leads and I is the identity matrix of dimension equal to the number of device lattice sites. In general, for a structure with N atoms, solving for all elements of the Green's function involves inverting an $N \times N$ matrix. Computational resources limit the size of the system that can be considered. However, by careful ordering of lattice sites the matrix corresponding to Eq. (2.5) is block tridiagonal [Eq. (2.6)].

$$\begin{pmatrix} A_1 & B_{12} & O & O & O & O & O \\ B_{21} & A_2 & B_{23} & O & O & O & O \\ O & B_{32} & \bullet & \bullet & O & O & O \\ O & O & \bullet & \bullet & \bullet & O & O \\ O & O & O & \bullet & \bullet & \bullet & O \\ O & O & O & O & \bullet & \bullet & B_{N-1N} \\ O & O & O & O & O & B_{N-1N} & A_N \end{pmatrix} \begin{pmatrix} G_{11}^r \\ G_{12}^r \\ \bullet \\ \bullet \\ \bullet \\ G_{1N-1}^r \\ G_{1N} \end{pmatrix} = \begin{pmatrix} 1 \\ O \\ O \\ O \\ O \\ O \\ O \end{pmatrix}. \tag{2.6}$$

For this purpose we divide the structure into smaller units, each unit typically representing one or a few rings of atoms along the circumference of the tube. The diagonal submatrix A_i (dimension of $N_i \times N_i$) represents $EI - H - \Sigma_L^r - \Sigma_R^r$ of the ith unit and the off-diagonal submatrix B_{ij} (dimension of $N_i \times N_j$) represents the coupling between units i and j, where N_i and N_j are the number of sites in units i and j. O are empty matrices. In the near-neighbor tight-binding scheme, B_{ij} is nonzero only when $|i-j| = 1$. Hence, there is a block tridiagonal structure for Eq. (2.5). Calculating the phase-coherent transmission coefficient involves only the off-diagonal component of the Green's function connecting the left and right ends of the device (G_{N1}^r). This further reduces the labor to compute the transmission coefficient. We solve for G_{N1}^r by using an efficient block tridiagonal elimination procedure. Using this procedure, we are able to calculate the transmission coefficient through long disordered regions.

The Green's function g_k^r is calculated via an iterative procedure.[24] The matrix equation corresponding to the semi-infinite leads is the same as Eq. (2.6), only that the matrix is semi-infinite, with all $A_i = A = E - H + i\eta$ (evaluated at a unit in lead k) and $B_{ij} = B_{ji}^t = B$. The equations for Γ_k and Σ_k^r involve only the submatrix $[g_k^r]_{11}$, which corresponds to the semi-infinite Green's function of the unit in lead k that is closest to the device region. From Eq. (2.6), $[g_k^r]_{11}$ is given by the following equation:[24]

$$[g_k^r]_{11} = \frac{I}{E - H + i\eta - B^t [g_k^r]_{11} B}. \tag{2.7}$$

The current across the device is calculated using the Landauer-Buttiker formula,

$$I = \frac{2e}{\hbar} \int dE T(E)[f_1(E) - f_2(E)], \tag{2.8}$$

where the factor 2 accounts for spin degeneracy. $f_1(E)$ and $f_2(E)$ are the Fermi functions of the waves incident from the two contacts to the device. Note that in the present work, we calculate only the phase-coherent transmission coefficient (the effect of electron-phonon interaction is neglected) and that temperature dependence is only via the Fermi factors of electrons. Two important considerations in a calculation of current are the equilibrium location of the Fermi level with respect to the band bottom of the device when connected to the contacts[25] and the self-consistent potential profile of the device in the presence of an applied bias. We assume the case of reflectionless contacts[20,26] and consider the scenario where the Fermi energy can be varied with respect to the band bottom of the CNT. The ability to vary the Fermi en-

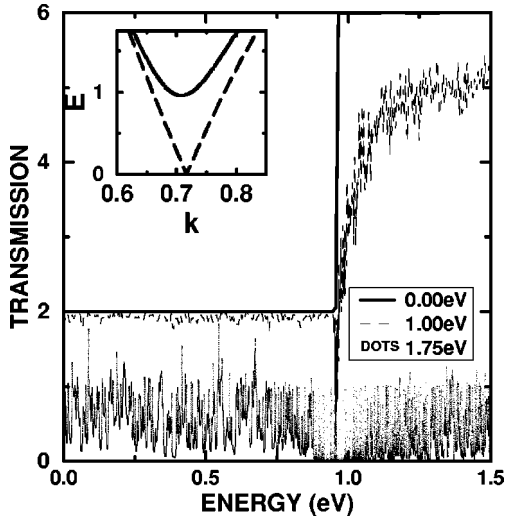


FIG. 2. Transmission versus energy for a (10,10) CNT with disorder distributed over a length of 1000 Å. The significant features here are the robustness of the transmission around the zero of energy, as the strength of disorder is increased, and the dip in transmission at energies close to the beginning of the second subband. The inset shows energy versus wave vector for the first (solid) and the second subband (dashed); the velocity of electrons at the minima of the solid line is zero.

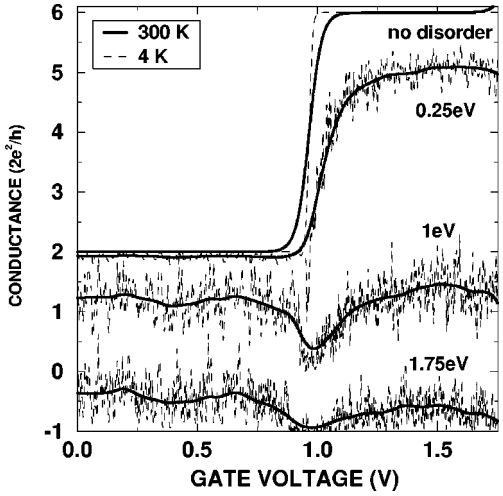


FIG. 3. The low bias conductance versus gate voltage for the structure used in Fig. 2. The figure clearly shows the dip in the conductance when the Fermi energy is close to the second subband minima. At the lower temperature, features due to the quasibound resonances in the disordered region are not averaged out when compared to the high-temperature case.

ergy in a CNT has been demonstrated experimentally in Refs. 3, 27, and 28. The potential in the device is not calculated self-consistently and we simply assume a linear drop in the applied potential, while calculating the current versus voltage characteristics.

III. RESULTS AND DISCUSSION

A. Weak uniform disorder

In a conventional one-dimensional chain, electrons traverse only a single effective path across the leads and as a result transmission is significantly altered by small amounts of disorder.[29] In comparison, electrons in a CNT can travel around defects because of the larger number of atoms in a cross section (the number of modes is only two at the band center). An important issue is how disorder affects the conductance of CNT wires. We calculate transmission (by this we mean the sum of the transmission coefficient over the incident modes, $\Sigma_n T_n$) as a function of both the length of the disordered region and the magnitude of disorder using the procedure described in Sec. II. Transmission versus energy and conductance versus gate voltage for one configuration of disorder are shown in Fig. 2. Transmission in a CNT has the following features that are in common with a single-moded one-dimensional chain: rapidly varying peaks that signify local resonances created by disorder and decrease in the average value with increasing disorder as the mismatch in the energies of the resonances increases with increase in disorder.[14,29]

We now discuss features that are typical of carbon nanotubes. Figure 2 shows a significant reduction in the transmission coefficient at energies close to the beginning of the second subband, even for weak disorder strengths. This leads to a dip in conductance when the Fermi level is close to the beginning of the second subband (Fig. 3). The origin of this dip is due to low velocity electrons in the second subband and can be understood as follows. In a perfect lattice, the velocity (dE/dk) of electrons with the quantum number of the second subband and with an energy close to the beginning of the second subband is nearly zero. These low-velocity electrons are easily reflected by the smallest of disorders. Disorder causes mixing of the first and second subbands. As a result, electrons incident in either subband at these energies develop a large reflection coefficient (in comparison to energies close to the band center). Increasing the disorder strength results in further reduction of the conductance and also results in the broadening of the dip. Subsequent to Eq. (2.2), we mentioned that the finite spatial extent of $\delta\epsilon_i$ is neglected in our study. A model that includes the finite spatial extent of $\delta\epsilon_i$ would require larger lengths of disordered regions to see dips whose magnitude is comparable to those in Figs. 2 and 3. The results in Fig. 2 are for one random configuration of disorder distributed over a length of 1000 Å. We have carried out simulations over different length scales and disorder configurations and our results for the average transmission at the band center, averaged over more than a thousand disorder configurations, are summarized in Fig. 4. The important point here is that for the smaller disorder strengths, the average transmission of a micrometer-long (10,10) tube is not significantly affected by disorder, thus demonstrating the relative robustness of transport at the band center. For disordered regions larger than some localization length (L_0), the conductance of quasi-one-dimensional samples has been predicted to decrease exponentially with length, $g = g_0 \exp(-L/L_0)$, in the phase-coherent limit.[14] For lengths shorter than the localization length, the decrease in conductance is not given by this equation. We observe this to be the case in our simulations (inset of Fig. 4). The values of L_0 corresponding to disorder strengths of 1 eV and 1.75 eV are 3353 Å and 1383 Å, respectively.

We also compute transmission for nanotubes of different diameters. This study illustrates the effect of the number of

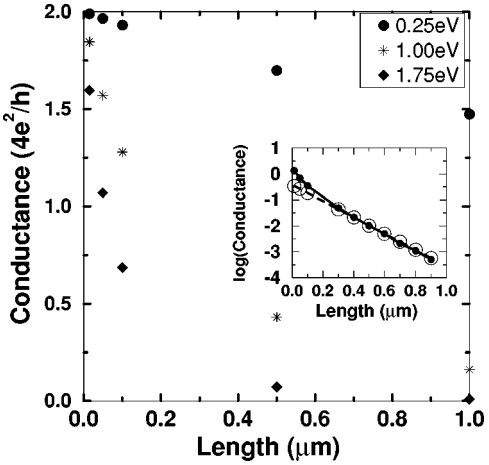


FIG. 4. The conductance versus length of the (10,10) CNT. While for the large disorder strengths the conductance is significantly affected by disorder, the conductance is reasonably large for the smaller values of disorder. This demonstrates the robustness of these wires to weak uniform disorder. Inset: log(Conductance) versus length for disorder strength of 1.75 eV in a (5,5) CNT. The solid line (filled circle) corresponds to the simulation and the dashed line (empty circle) corresponds to that obtained using $g = g_0 \exp(-L/L_0)$.

atoms in a cross section of the wire. We compare transmission of the (10,10) tube with that of (5,5) and (12,0) zigzag tubes. The diameters of these tubes are 13.4 Å, 9.4 Å, and 6.7 Å, respectively. For the (10,10) and (5,5) tubes, the band structures at energies close to the Fermi energy are similar.[21] But the number of atoms in a unit cell of a (5,5) tube is only half of that in a (10,10) tube (they have 20 and 40 atoms, respectively). Figure 5 shows the average transmission versus wire length. The important point here is that in spite of the identical transmission of a disorder-free (10,10) and (5,5) tube at energies around the band center, transmission is smaller for the (5,5) tube in the presence of disorder. This is because the (5,5) tube has a smaller number of atoms around

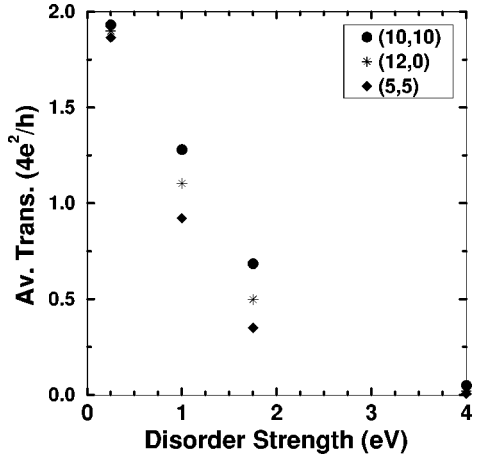


FIG. 5. The average transmission at the band center versus disorder strength for wires of different diameter and chirality; the transmission has been averaged over a thousand different realizations of the disorder. The main feature here is that the average transmission decreases with a decrease in the number of atoms along the circumference of the wire (see text).

the circumference, thus reducing the number of paths by which electrons can travel around defects and across the device. To support this viewpoint, we compare these results to conductance of a 1000 Å long (12,0) zigzag tube. We find that transmission is in between that of the (10,10) and (5,5) tubes (Fig. 5). This is because the (12,0) tube has a diameter that is in between that of the (10,10) and (5,5) tube, and as a result the number of effective paths is larger than that available to a (5,5) tube but smaller than that of a (10,10) tube.

Recently, arm chair, zigzag, and tubes with chiralities in between have been experimentally characterized by STM imaging.[30,31] Transport measurements of single-wall CNT at low temperatures have so far been limited by Coulomb blockade due to large barriers at the contact-CNT interface.[3,27] Disorder of some degree is bound to exist in CNT samples and we believe that the variation in the linear-response conductance with the gate potential[32] and the dip in the conductance at energies close to the crossing of the first and second subbands can be observed in situations where the contact resistance is not the dominant factor. The length dependence of the conductance can also be studied by varying the length of the tube between the electrodes. One caveat is that phonon scattering will cause an increase in the low bias conductance in the presence of strong disorder with an increase in temperature. Our calculations are relevant at low temperatures where phonon scattering is not significant.

B. Strong isolated defects

An electron cannot hop on to such a defect site either due to a large mismatch in the on-site potential or weak bonds with its neighbors (Sec. II). Scattering from a single defect causes a maximum reduction in the transmission at the band center $E = 0$. For example, the transmission of a (10,10) tube reduces from 2 to approximately 0.94 due to a single defect.[5] We are interested in the effect of a few such defects scattered randomly along the length of the tube. Reflection from more than a single defect causes the creation of quasibound states along the tube, the exact locations of which are sensitive to the position of the defects. We find that a significant feature that is independent of the exact location of these defects is the opening of a *transmission gap* at the center of the band as defects are added. The second feature that we see in the simulations is that the width of the transmission gap increases with an increase in the defect density. The transmission has sharp decreases at energies corresponding to the opening of the second subband, but this effect is relatively weak compared to the previous case of disorder. The simulation results illustrating these features are shown in Figure 6 for a wire of length 1000 Å with ten defects scattered along the length randomly. As a result of the transmission gap, the low bias conductance is greatly reduced from the defect-free case, at zero gate voltage. Conductance further depends significantly on temperature [inset of Fig. 7(a)]. In summary, while the conductance is not significantly affected by relatively weak uniform disorder (Figs. 3 and 4), we find that the conductance here is much smaller than $2e^2/h$ at zero gate voltage. Conductance increases with gate voltage, with features of resonances due to the quasibound states superimposed. These features get averaged out with an increase in temperature. We also calculate current as a function of applied voltage by assuming a linear drop in the applied volt-

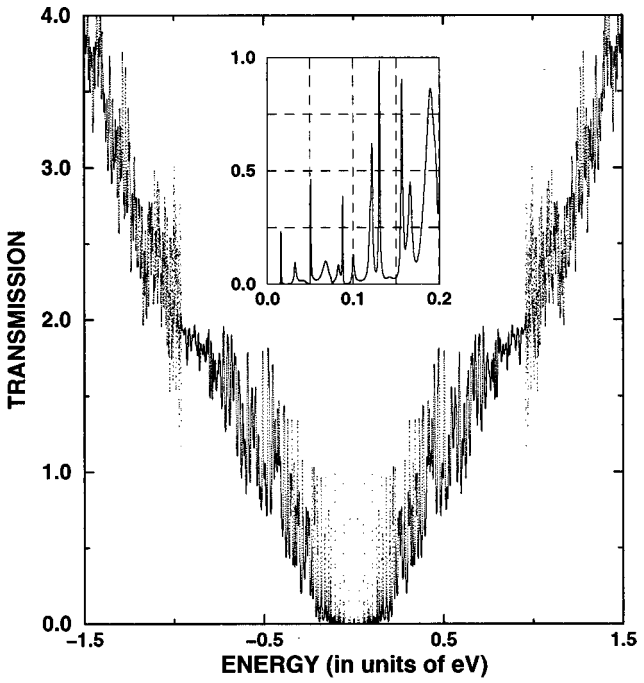


FIG. 6. The transmission versus energy for a (10,10) CNT with ten strong isolated scatterers sprinkled randomly along a length of 1000 Å. The main prediction here is the opening of a transmission gap around the zero of energy. Inset: Comparison of the transmission for tubes of lengths 1000 Å (solid) and 140 Å (dashed) with ten scatterers in each case. The transmission gap is larger for the larger defect density and the sharp resonances close to the zero of energy are suppressed with increasing defect density.

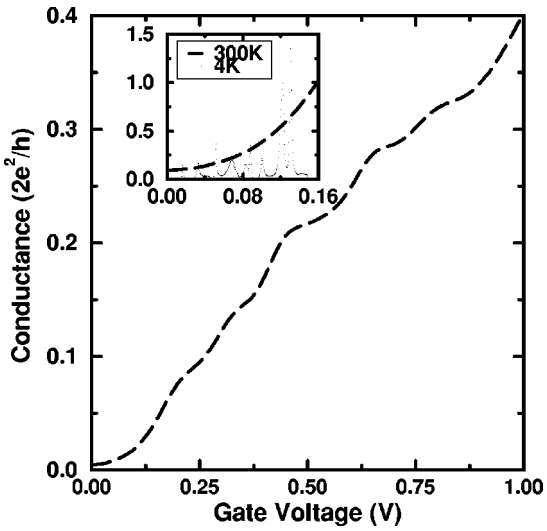


FIG. 7. The conductance at $T = 300$ K for the case in Fig. 6. The low conductance at zero gate bias represents the transmission gap in Fig. 6. The transmission resonances of Fig. 6 get averaged out here. The inset compares the effect of temperature on the conductance. Close to zero gate voltage, the conductance is clearly suppressed at the lower temperature.

age. Transmission at each applied voltage is computed and then we use Eq. (2.8) to calculate the current. The main feature in the I-V characteristic is the small increase in current with applied voltage close to the zero of applied voltage (Fig. 8). The experimental work in Ref. 4 measured the I-V characteristics of a CNT rope. One of their main findings was that the differential conductance is very small at zero bias and that it increases with an increase in applied bias. The qualitative features of Fig. 8 are similar but an important difference is that the experiments were performed on a rope of single-walled tubes, in which case it has recently been predicted that a band gap could open due to tube-tube interactions.[33]

IV. CONCLUSIONS

We present a method to calculate the phase-coherent transmission through nanotubes using a Green's-function formalism that can include the effect of semi-infinite leads and can handle many defects and junctions with relative ease. We use this formalism to study the importance of scattering due to disorder. Two simple models of disorder are considered and their effect on the conductance is discussed. In the presence of weak uniform disorder, we find that the conductance is not significantly affected by disorder and that the wires behave as reasonably good quantum wires. For example a micrometer-long (10,10) CNT with a disorder strength of 1 eV (section II) has a conductance comparable to $0.16(e^2/h)$. We predict that an experiment involving measurement of conductance versus gate voltage will show a dip in conductance when the Fermi energy is close to the opening of the second subband (Fig. 3). We compare the conductance of wires with varying diameters and find that the transmission (conductance) increases with the diameter of the tube for a given disorder strength (Fig. 5; note that in the absence of disorder the conductance is independent of the tube diameter at zero gate voltage). We attribute this to a decrease in the number of effective paths by which an electron can traverse across the device with a decrease in the diameter. The second type of defect considered is strong isolated scatterers. In contrast to the previous type of disorder, this disorder creates a gap in the transmission at the band

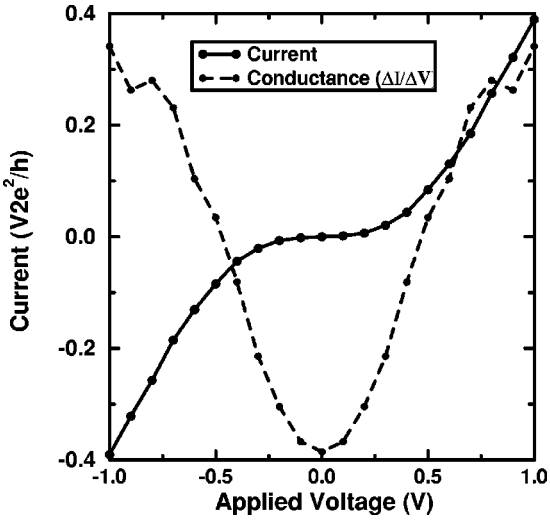


FIG. 8. The current (shifted by -0.4 units along the current axis) versus applied voltage for the same structure as in Fig. 6. The dashed curve is the differential conductance, which is very small at low applied voltages.

center and a corresponding large reduction in the low bias conductance. Such disorder would destroy the good conductance properties of the wire at the band center. The work presented is based on numerical simulations. Of interest could be further conductance experiments to look for features described in this paper. Carbon nanotubes provide an unprecedented natural scenario for wires with a few modes and a relatively small cross-sectional area. An analytical study of the effect of disorder in these systems and the dependence of the conductance as a function of diameter and chirality would be useful. Also of interest for future work would be a study that includes the effect of phonon scattering.

We would like to thank Jie Han (NASA Ames Research Center) for sharing his expertise on many aspects of carbon nanotubes and for lively discussions. We would like to thank Manoj Samanta and Supriyo Datta of Purdue University for communicating the result of [Eq. (2.7)] before publication.[24] It is also a pleasure to acknowledge useful discussions with Supriyo Datta (Purdue University) and Mathieu Kemp (Northwestern University).

*Author to whom correspondence should be addressed, Electronic address: anant@nas.nasa.gov

†Electronic address: tr@nas.nasa.gov

[1] H. Dai, J. H. Hafner, A. G. Rinzler, D. T. Colbert, and R. E. Smalley, Nature (London) **384,** 147 (1996).

[2] W. A. der Heer, A. Chatelain, and D. Ugarte, Science **270,** 1179 (1997).

[3] S. J. Tans, M. Devoret, H. Dai, A. Thess, R. E. Smalley, L. J. Geerligs, and C. Dekker, Nature (London) **386,** 474 (1997).

[4] P. G. Collins, A. Zettl, H. Bando, A. Thess, and R. E. Smalley, Science **278,** 100 (1997).

[5] L. Chico, V. H. Crespi, L. X. Benedict, S. G. Louie, and M. L. Cohen, Phys. Rev. Lett. **76**, 971 (1996).

[6] L. Chico, L. X. Benedict, S. G. Louie, and M. L. Cohen, Phys. Lett. B **54**, 2600 (1996).

[7] R. Saito, G. Dresselhaus, and M. S. Dresselhaus, Phys. Rev. B **53**, 2044 (1996).

[8] R. Tamura and M. Tsukada, Phys. Rev. B **55**, 4991 (1997).

[9] H. Lin, Phys. Rev. B **58**, 4960 (1998).

[10] R. Egger and A. O. Gogolin, Phys. Rev. Lett. **79,** 5082 (1997).

[11] C. Kane, L. Balents, and M. P. A. Fisher, Phys. Rev. Lett. **79**, 5086 (1997).

[12] L. Balents and M. P. A. Fisher, Phys. Rev. B **55**, 11 973 (1997).

[13] Yu. A. Krotov, D.-H. Lee, and S. G. Louie, Phys. Rev. Lett. **78**, 4245 (1997).

[14] C. W. J. Beenakker, Rev. Mod. Phys. **69,** 731 (1997), and references therein.

[15] D. Zhou and S. Seraphin, Chem. Phys. Lett. **238,** 286 (1995).

[16] J. Lu and J. Han, in *Carbon Nanotubes and Nanotube Based Nanodevices*, in *Quantum-based Electronic Devices and Systems,* edited by P. K. Tien *et al.* (World Scientific, Singapore, 1998).

[17] M. Menon and D. Srivastava, Phys. Rev. Lett. **79**, 4453 (1997).

[18] C. Caroli, R. Combescot, P. Nozieres, and D. Saint-James, J. Phys. C **4**, 916 (1971).

[19] Y. Meir and N. S. Wingreen, Phys. Rev. Lett. **68,** 2512 (1992).

[20] S. Datta, *Electronic Transport in Mesoscopic Systems* (Cambridge University Press, Cambridge, UK, 1995).

[21] M. S. Dresselhaus, G. Dresselhaus, and P. C. Eklund, *Science of Fullerenes and Carbon Nanotubes* (Academic Press, New York, 1996), Chap. 19.

[22] J.-C. Charlier, T. W. Ebbesen, and Ph. Lambin, Phys. Rev. B **53,** 11 108 (1996).

[23] S. G. Louie, in *Proceedings of the Robert A. Welch Foundation, 40th Conference on Chemical Research, Chemistry on the Nanometer Scale, Houston, 1996* (Welch Foundation, Houston, 1996).

[24] M. P. Samanta and S. Datta, Phys. Rev. B **57,** 10 972 (1998).

[25] S. Datta, W. Tian, S. Hong, R. Reifenberger, J. I. Henderson, and C. P. Kubiak, Phys. Rev. Lett. **79,** 2530 (1997).

[26] E. Tekman and S. Ciraci, Phys. Rev. B **43**, 7145 (1991).

[27] M. Bockrath, D. H. Cobden, P. L. McEuen, N. G. Chopra, A. Zettl, A. Thess, and R. E. Smalley, Science **275,** 1922 (1997).

[28] A. Bezryadin, A. R. M. Verschreren, S. J. Tans, and C. Dekker, Phys. Rev. Lett. **80,** 4036 (1998).

[29] J. Ziman, *Models of Disorder: The Theoretical Physics of Homogeneously Disordered Systems* (Cambridge University Press, Cambridge, UK, 1979).

[30] J. W. G. Wildoer, L. C. Venema, A. G. Rinzler, R. E. Smalley, and C. Dekker, Nature (London) **391**, 59 (1998).

[31] T. W. Odom, Jin-Lin Huang, P. Kim, and C. M. Lieber, Nature (London) **391,** 62 (1998).

[32] The gate potential causes the Fermi energy of the CNT to shift with respect to its band bottom.

[33] P. Delaney, H. H. Choi, J. Ihm, S. F. Louie, and M. L. Cohen, Nature (London) **391**, 466 (1988).